Dephasing effects in a two-dimensional magnetic-breakdown linked-orbit network: Magnesium

J. K. Freericks and L. M. Falicov
Department of Physics, University of California, Berkeley, California 94720
and Materials and Chemical Sciences Division, Lawrence Berkeley Laboratory, Berkeley, California 94720
(Received 2 November 1988)

The galvanomagnetic properties of a magnetic-breakdown linked-orbit network with two-dimensional topology are calculated for the case of a stochastic distribution of defects in the network. The results show excellent agreement with experiments on magnesium and illustrate the transition between a smoothly varying magnetoresistivity (semiclassical regime) and an oscillatory magnetoresistivity (quantum regime).

I. INTRODUCTION

We examine the dephasing effect of dislocations (and other defects) on electron transport in metals which exhibit magnetic breakdown (MB). The phenomenon of MB was introduced in 1961 by Cohen and Falicov[1] to explain the "giant orbit" observed in de Haas–van Alphen experiments in magnesium. Since then, the concept of MB has been applied to many experimental situations involving the dynamics of electrons in magnetic fields (for a review see Ref. 2). The effect of MB is to alter the topology (or character) of electron (or hole) orbits by a tunneling mechanism that, probabilistically, couples orbits together. Its importance lies in the extremely sensitive dependence of these coupling probabilities to magnetic field strength and orientation.

The manner in which MB manifests itself in a given sample is strongly correlated with the density of dislocations.[3] The presence of dislocations breaks the periodicity of the lattice and produces small changes in the areas of some closed orbits. This results in a reduction of the quantum coherence of the electronic wave functions. For high dislocation densities the coherence is completely lost and the transverse magnetoresistivity is a smoothly varying function of the magnetic field strength that, at high fields, either saturates or increases quadratically with the field. For low dislocation densities the coherence of the electronic wave functions over small closed orbits modulates the coupling probabilities and leads to quantum oscillations in the magnetoresistance (a giant Shubnikov–de Haas effect), with phases of the oscillations proportional to the magnetic flux enclosed by the phase-coherent closed orbits of the network. This transition from semiclassical to quantum behavior suggests the possibility of using measurements of the magnetoresistance to determine the stochastic distribution of dislocations and observe their effect on the coherence of the electronic wave functions. In this contribution we study the dephasing effect of dislocations in a two-dimensional hexagonal network and compare our theory with experimental results[2] for Mg. Similar studies have been made for the linear chain[4] and applied to observations[5] in $NbSe_3$.

Sowa and Falicov[4] solved the one-dimensional network model exactly (in the infinite–relaxation-time limit) by iterating 2×2 transfer matrices. Similar transfer-matrix techniques, applied to the two-dimensional network, are cumbersome to handle and fail to yield closed-form solutions. We have developed here a rapidly convergent approximation scheme which models the effects of dislocations and allows for numerical solutions and direct comparison with experiment.

The semiclassical electronic orbits in a magnetic field are defined by the intersection of surfaces of constant energy (the Fermi surface) with planes of constant wave-vector components in the direction parallel to the field.[6] At low temperatures, only electrons at the Fermi surface can contribute to the conductivity. Two components of the Fermi surface are of interest in the divalent hexagonal-close-packed metals: (1) the multiply connected region in the second Brillouin zone (BZ) that contains holes (usually called the "monster"); (2) the singly connected electron surfaces centered around the K point in the third BZ (usually called "cigars" or "needles"). In the absence of MB, the only possible relevant orbits in the $k_z=0$ plane are the holelike hexagonal orbit of the second BZ and the two electronlike triangular orbits of the third BZ. In the presence of MB, an electron wave packet that approaches a junction is either Bragg diffracted or tunnels across the gap into the next BZ. In this manner, MB links the hexagonal and triangular oribits into the hexagonal network of Fig. 1. For intermediate fields many orbits are possible—when MB is complete, only the free-electron-like circle is present. It is this transition from the dominating holelike hexagonal orbit to the electronlike circle which destroys the electron-hole compensation of these metals and causes the transverse magnetoresistivity to saturate[6]—were it not for MB the transverse magnetoresistance would increase quadratically without any bound.

Our approach to modeling the influence of dislocations on the galvanomagnetic tensors begins with the idealized model of Pippard,[7] where one treats the orbits as a network with MB switching junctions at points of intersection. This model is justified by the fact that in a metal the electronic wave functions are localized on a "racetrack" with a width much narrower than the radius of the track.[8] Within this model, the most important ele-

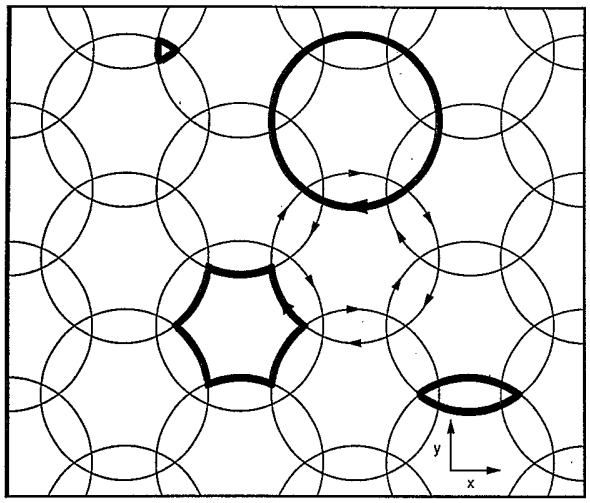

FIG. 1. Two-dimensional MB linked-orbit hexagonal network in real space. The triangular, lens, hexagonal, and circular orbits are highlighted.

ment is the length scale over which the electronic wave functions maintain their quantum-mechanical phase coherence. When coherence is important, the MB junctions are treated as quantum-mechanical switches, in which a wave packet of unit amplitude and zero phase splits according to the quantum packets of Fig. 2. There H is the magnetic field and H_0 is the MB field (for justification of the basic MB formulas see Ref. 2). We work in the infinite–relaxation-time limit, neglecting all other scattering mechanisms (phonons, impurities, etc.) besides MB itself. In this approximation, the probability amplitude remains constant and the phase changes by the standard line integral of the vector potential[7] as the electron traverses the circular arc between two junctions.

Small-angle scattering effects which do not affect the probability amplitude but tend to randomize the phase are taken into account as follows:[3,9] we assume that the phase is completely randomized over all orbits except for the small triangular orbits where phase coherence may or may not be maintained. In this limit, the hexagonal network of Fig. 1 reduces to a network of "touching" circles [see Fig. 3(a)] with three-way nodes whose coupling probabilities—R, S, and $T=1-R-S$—determine the allowed exit paths for an entering wave packet of unit amplitude [see Fig. 3(b)]. Total loss of coherence is assumed on this effective network, so that only the probability amplitude of a wave packet is important (extensions of this approximation to allow for coherence over larger orbits has been considered in Ref. 10).

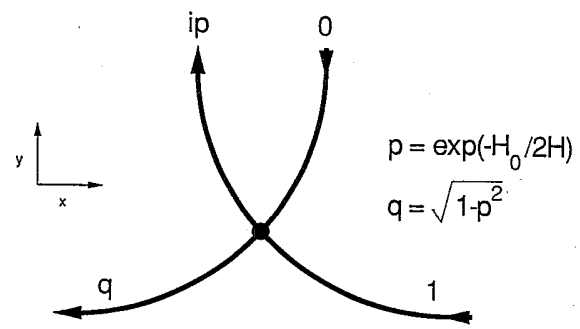

FIG. 2. A magnetic-breakdown junction: probability amplitudes and phases.

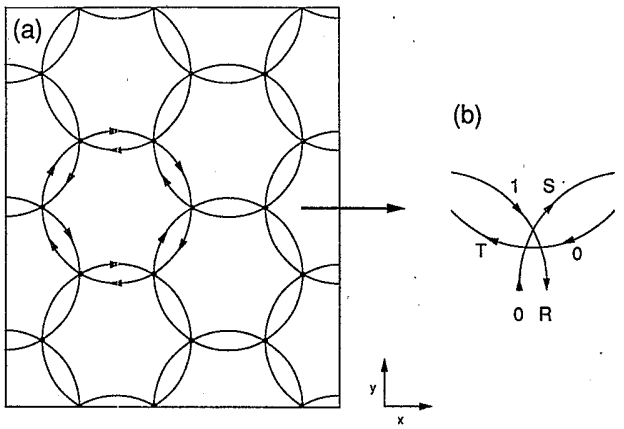

FIG. 3. Effective MB linked-orbit network with triangle-orbit area shrunk to zero. (a) Network with three-way switching nodes. (b) Coupling probabilities for a node.

The coupling probabilities of Fig. 3(b) are evaluated in the quantum limit (total coherence over the triangular orbit) as follows: a wave packet of unit amplitude is injected into one of the three incoming channels and allowed to circulate the infinitesimal triangular orbit. As the packet leaks out onto the three outgoing channels, the contributions to the probability amplitude for each channel are summed (for a complete derivation see the appendix of Ref. 3). The absolute square of the total amplitude yields the coupling probabilities

$$R(\theta)=\frac{p^4}{1-2q^3\cos\theta+q^6}\,,$$
$$S(\theta)=\frac{q^2(1-2q\cos\theta+q^2)}{1-2q^3\cos\theta+q^6}\,, \tag{1}$$
$$T(\theta)=\frac{p^4q^2}{1-2q^3\cos\theta+q^6}\,,$$

with θ the phase change of the electronic wave function for one circuit of the triangular orbit. Since this phase change is simply the magnetic flux through the orbit, we find

$$\theta=A_k\frac{\hbar c}{eH}+\text{const}\,, \tag{2}$$

where A_k is the k-space area of the triangular orbit. In the semiclassical limit (no phase coherence over the triangular orbit) the phase is uniformly randomized over the interval $[0,2\pi]$, yielding the semiclassical result

$$R_c\equiv\frac{1}{2\pi}\int_0^{2\pi}d\theta\,R(\theta)=\frac{p^4}{1-q^6}\,,$$
$$S_c=\frac{q^2(1+q^2-2q^4)}{1-q^6}\,, \tag{3}$$
$$T_c=\frac{p^4q^2}{1-q^6}\,,$$

for the coupling probabilities. The low-field limit ($H\to 0, q\to 1, S\to 1$) yields unit probability for the hexagonal orbit and the high-field limit ($H\to\infty$, $q\to 0, R\to 1$) yields unit probability for the circular orbit, as expected. The pure lens orbit, corresponding to $T\to 1$ (see Fig. 1), is not physically accessible with unit probability, but it does have a finite probability for intermediate magnetic fields.

In the next section we use R, S, and T to calculate the galvanomagnetic tensors of the hexagonal network of Fig. 3(a). We allow for dislocations (in the quantum regime) by assuming a stochastic distribution of the triangular-orbit area A_k and taking ensemble averages of the observables over the probability distribution for these areas. In Sec. III we apply our theoretical model to Mg. Conclusions are presented in the final section.[11]

II. GALVANOMAGNETIC TENSORS AND THE EFFECTIVE-PATH MODEL

The effective-path model of Pippard[3,9] is used to calculate the galvanomagnetic tensors. When an electric field $\mathbf{E}$ is applied to a metal, it causes a Fermi-surface element $d\mathbf{S}$ to be displaced, sweeping out a volume $e\mathbf{E}\cdot d\mathbf{S}/\hbar$ in $\mathbf{k}$ space per unit time. This process is interpreted as the creation of quasiparticle packets, of average vector $\mathbf{k}$, that are subsequently scattered as they move through the metal, traveling an average distance $\mathbf{L}(\mathbf{k})$ after creation. This distance $\mathbf{L}(\mathbf{k})$ is called the *effective path*. The current $\mathbf{J}$ set up by the electric field is then

$$\mathbf{J}=\frac{e^2}{4\pi^2\hbar}\int \mathbf{L}(\mathbf{E}\cdot d\mathbf{S}) , \tag{4}$$

with the integral extending over the Fermi surface. The solution for $\mathbf{L}(\mathbf{k})$ is simplified in the infinite-relaxation-time limit, where the only scattering process considered is caused by MB itself. In this limit the effective path is completely determined as a function of the MB coupling probabilities R, S, and T. Moreover, since we neglect scattering on the circular arms of the effective network in Fig. 3(a), the effective path may be written as

$$\mathbf{L}_b(\mathbf{k})=\mathbf{\Lambda}_b-\mathbf{X}_b(\mathbf{k}) , \tag{5}$$

where b refers to a specific branch of the network, $\mathbf{\Lambda}_b$ is the center of mass of the probability distribution as $t\to\infty$ of an electron packet originating on the b branch, and $\mathbf{X}_b(\mathbf{k})$ is the initial (real-space) position of the electron packet at creation.

Probability conservation at a node relates to each other the centers of mass of packets at different branches. For example, we find

$$\mathbf{\Lambda}_1=R(\alpha)\mathbf{\Lambda}_2+S(\alpha)\mathbf{\Lambda}_3+T(\alpha)\mathbf{\Lambda}_4 \tag{6}$$

for the node labeled α in Fig. 4. If the crystal is periodic, then R, S, and T are independent of the node index α and the $\mathbf{\Lambda}_b$ are related to one another by simple rotations and/or translations.[2,3] The algebraic equation (6) is then easily solved relative to the origin of Fig. 4, yielding the perfect-crystal result

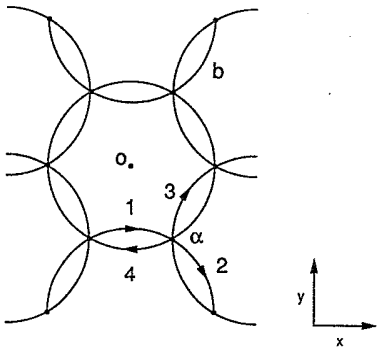

$$\Lambda_1 = R(\alpha)\,\Lambda_2 + S(\alpha)\,\Lambda_3 + T(\alpha)\,\Lambda_4$$

FIG. 4. Detail of the effective hexagonal network. The origin is the center of one particular free-electron circle. A particular node is labeled by α and the adjacent branches are labeled by integers; b denotes an arbitrary branch in the network.

$$\frac{\mathbf{\Lambda}_1}{r}=\frac{3(R+S-R^2-RS-S^2)-i\sqrt{3}[4-5R-7S+3(R^2+RS+S^2)]}{8-12(R+S)+6(R^2+RS+S^2)} , \tag{7}$$

where r is the free-electron-circle radius and where we have used the complex-number notation $\mathbf{A}=A_x+iA_y$ for the two-dimensional vector $\mathbf{A}$.

The presence of dislocations in a metal introduces a small variation in the area of the triangular orbit from one node to another. This, in turn, generates fluctuations in the coupling probabilities (1), which break the periodicity and symmetry of the network and destroy the simple symmetry between the various $\mathbf{\Lambda}_b$.

Our approach to solving this problem is to introduce an ensemble of networks in which the k-space area of a dislocated orbit obeys a stochastic distribution, and to develop an approximation scheme to solve for the ensemble-averaged centers of mass. A Markovian process is assumed so that the stochastic distribution of probabilities at each node is independent of all other nodes. The approximation scheme begins by generalizing the $N=1$ probability conservation equation (6) to $N>1$ and relating the center of mass of a packet at branch 1 in Fig. 4 to the centers of mass of packets at every branch b linked to branch 1 by an orbit scattering through N (not necessarily distinct) nodes. The result is an equation of the form

$$\mathbf{\Lambda}_1=\sum_b P^N(b)\mathbf{\Lambda}_b , \tag{8}$$

where the branch probability $P^N(b)$ is the sum over all

paths—connecting branch 1 to branch b that pass through N nodes—of the product of the relevant coupling probability from each node along the path. The N-node probability conservation equation (8) is ensemble averaged

$$\langle \Lambda_1 \rangle = \sum_b \langle P^N(b) \rangle \langle \Lambda_b \rangle \tag{9}$$

to restore periodicity, since the ensemble-averaged centers of mass $\langle \Lambda_b \rangle$ are related to each other by the symmetry operations of the network. This method reduces the solution for the ensemble-averaged effective path, by means of (5), to the solution of a simple algebraic equation.

The approximation scheme outlined above is exact in two limits: (1) when there are no dislocations (the stochastic distribution is a single delta function), then periodicity is never lost, the ensemble averaging is trivial $\langle R^l S^m T^n \rangle = R^l S^m T^n$ and the center of mass reduces to the perfect crystal result (7) for all N; (2) as $N \to \infty$ all possible paths which link a branch b to branch 1 are taken into account, thus yielding also an exact result. We have found, however, that the approximation converges rapidly in N for any reasonable distribution, and have used the $N=8$ approximation in the work that follows. The results for $\langle \Lambda_1/r \rangle$ in the $N=1$ and $N=2$ approximations are the perfect-crystal result (7), with the replacement $R^m \to \langle R \rangle^m$ and $S^m \to \langle S \rangle^m$ for any m. The calculations for higher N are straightforward but tedious, since the number of paths considered at each level of the approximation increases exponentially with N.

In actual experimental samples the small triangular orbits of Fig. 1 lose phase coherence in low magnetic fields. This loss of coherence requires an interpolation between the semiclassical regime [where the center of mass Λ_1^c is expressed by (7) with $R \to R_c$ and $S \to S_c$ of Eq. (3)] and the quantum regime (where the center of mass Λ_1^q is determined by the ensemble averaging described above) in our effective-network model. Following Ref. 10 a coherence field $H_{\rm coh}$ is introduced; it depends on the density of dislocations. The coherence field is treated as an experimental fit parameter that increases with increasing dislocation density. It determines the weighting factor for the quantum regime by

$$w_q(H) = e^{-(H_{\rm coh}/H)^2} . \tag{10}$$

The weighting factor for the semiclassical regime is $w_c(H) = 1 - w_q(H)$. The result is an effective center of mass

$$\Lambda_1^{\rm eff}(H) = w_c(H)\Lambda_1^c + w_q(H)\Lambda_1^q \tag{11}$$

which, when replaced in (5), yields the desired effective path.

The conductivity tensor σ_{ij} is determined from (4) by an integration over the Fermi surface. However, the final result is modified to incorporate electron-hole compensation at $H=0$, which is characteristic of the divalent hexagonal-close-packed metals. The magnetoconductivity is then[3]

$$\sigma_{xx} = \sigma_{yy} = \frac{3nec}{\pi H} \mathrm{Re}(\Lambda_1^{\rm eff}) , \tag{12a}$$

$$\sigma_{xy} = -\sigma_{yx} = \frac{3nec}{\pi H} \mathrm{Im}(\Lambda_1^{\rm eff}) , \tag{12b}$$

where n is the density of electrons in the metal. The magnetoresistivity tensor is found by inversion.

III. DEPHASING EFFECTS IN MAGNESIUM

In this section, the theory developed above is applied to electron transport in magnesium by comparing model calculations for the transverse magnetoresistivity with the experimental results.[2] The MB field and the k-space area of the triangular orbit,

$$H_0 = 5.85 \text{ kG}, \quad A_k = 6.49 \times 10^{-3} \text{ a.u.} , \tag{13}$$

have been determined[9] for Mg, while the number density,

$$n = 6.9 \times 10^{21} \text{ cm}^{-3} , \tag{14}$$

is determined from the scale of the experimental data.

The presence of dislocations introduces a stochastic distribution for the k-space area of the triangular orbit. Since a dislocated orbit has an area smaller than the true triangular orbit, we expect the distribution to be asymmetric with a peak about A_k and a tail extending toward smaller values $A < A_k$. This distribution is approximated by a delta function of weight μ at $A = A_k$ and a rectangular distribution of weight $(1-\mu)$ extending from λA_k to A_k $(\lambda < 1)$ so that the average value of any quantity O

$$\langle O \rangle = \mu O(A_k) + \frac{1-\mu}{(1-\lambda)A_k} \int_{\lambda A_k}^{A_k} O(A)\, dA , \tag{15}$$

is a function of the two parameters μ and λ.

The approximation scheme of the preceding section converges rapidly with N. To illustrate this, we have plotted in Fig. 5 the $N=1$ and $N=8$ approximations for a pure rectangular distribution ($\mu=0$) between $0.95A_k$ and A_k (the dashed line is an interpolation between the high-field region, where MB is the only important scattering mechanism, and the low-field region, where large-angle scattering effects corresponding to a finite-relaxation time are important). Comparison of these two graphs shows that the convergence is indeed very rapid. The $N=8$ approximation is used exclusively in the rest of this contribution.

The high dislocation density limit ($\mu=0$, $\lambda<0.5$) completely randomizes the quantum-mechanical phase (2), reproducing the semiclassical result (see Fig. 6) with no quantum oscillations. The magnetoresistivity depends only weakly on the parameter λ in this case.

The intermediate regime ($\mu \approx 0.1$, $\lambda \approx 0.9$) is strongly dependent on the parameters of the distribution. This case is illustrated in Fig. 7 and is in excellent agreement with the experimental results.[2]

The low dislocation density limit ($\mu \approx 0.9$, $\lambda \approx 0.9$) is the extreme quantum regime and once again it depends weakly on the distribution parameters. A typical case is shown in Fig. 8. This regime does not agree as well with experiment because the samples are so pure that phase

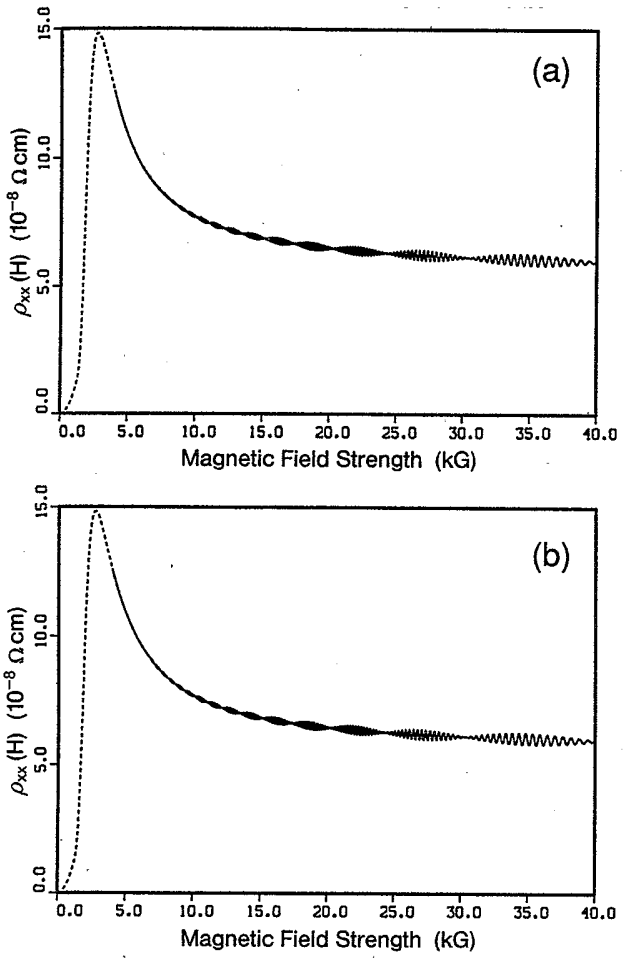

FIG. 5. Calculated transverse magnetoresistivity for Mg. The distribution of triangle-orbit areas is a rectangular distribution stretching from $0.95A_k$ to A_k ($\mu=0.0$, $\lambda=0.95$, $H_{coh}=10$ kG). (a) The $N=1$ approximation. (b) The $N=8$ approximation.

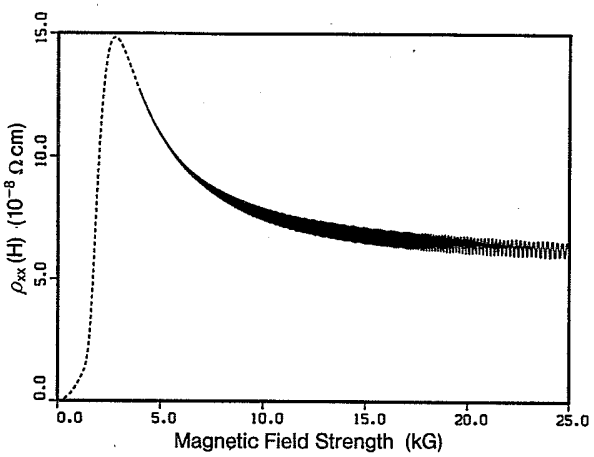

FIG. 7. Calculated transverse magnetoresistivity for Mg in the intermediate regime, with parameters $\mu=0.15$, $\lambda=0.85$, $H_{coh}=12$ kG.

coherence over orbits larger than the triangle are important.[10]

There are several important features apparent in Figs. 5–8. The presence of dislocations reduces the amplitude of the magnetoresistance oscillations because of a partial randomization of the quantum-coupling probabilities. As the density of dislocations increases, the randomization becomes complete; the semiclassical curve results. The envelope of the oscillations is modulated by a small amplitude oscillatory function at low dislocation density which resembles a beat structure. Beats do develop as the density of dislocations is increased due to the interference of oscillations at nearly equal frequencies. Both the oscillatory envelope and beat structure tend to be washed out in the experimental data. This is probably due to the fact that the real stochastic distribution is smoother than the rectangular one assumed here.

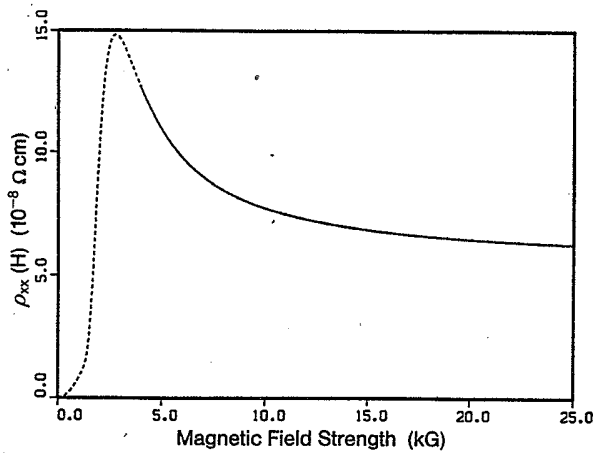

FIG. 6. Calculated transverse magnetoresistivity for Mg in the semiclassical regime, with parameters $\mu=0.0$, $\lambda=0.25$, $H_{coh}=15$ kG.

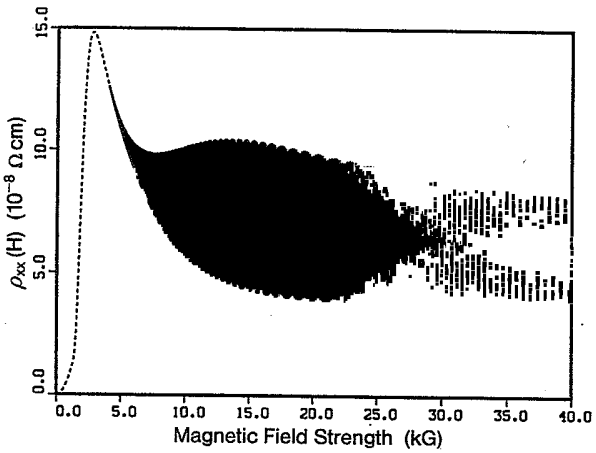

FIG. 8. Calculated transverse magnetoresistivity for Mg in the extreme quantum regime, with parameters $\mu=0.95$, $\lambda=0.95$, $H_{coh}=10$ kG.

IV. CONCLUSION

The problem of modeling the effect of dislocations (and other defects) on the transport properties of metals that exhibit MB has been an open problem for over a quarter of a century. We have presented a model calculation of the dephasing effect of dislocations on electron transport in a two-dimensional hexagonal network. An ensemble of equivalent networks is introduced and stochastic averages of observables over this ensemble are taken to restore periodicity to the system and allow for an accurate, but approximate, calculation of the galvanomagnetic tensors by the effective-path approach. In this way, we are able to show the transition from the semiclassical to the extreme quantum regimes as a function of the stochastic distribution of the triangular-orbit area which is a function of the density of dislocations.

The important result to emphasize is that the loss of oscillatory behavior of the galvanomagnetic properties is lost not by the quantum-to-semiclassical transition of each individual (triangular) orbit, but by destructive interference between various junctions caused by the random distribution of dislocations.

Our theoretical model has been compared with the experimental results for Mg and shows excellent agreement. In particular, the transverse magnetoresistivity is found to be very sensitive to the distribution of dislocations in the region intermediate between the semiclassical and extreme quantum regimes. The results can be used to determine accurately the dislocation distribution of given samples.

ACKNOWLEDGMENTS

One of the authors (J.K.F.) acknowledges partial support by the National Science Foundation. This research was supported, at the Lawrence Berkeley Laboratory, by the Director, Office of Energy Research, Office of Basic Energy Sciences, Materials Sciences Division, U.S. Department of Energy, under Contract No. DE-AC03-76SF00098.

[1]M. H. Cohen and L. M. Falicov, Phys. Rev. Lett. **7**, 231 (1961).

[2]R. W. Stark and L. M. Falicov, in *Progress in Low Temperature Physics,* edited by C. J. Gorter (North-Holland, Amsterdam, 1967), Vol. 5, p. 235.

[3]A. B. Pippard, Proc. R. Soc. London, Ser. A **287**, 165 (1965).

[4]E. C. Sowa and L. M. Falicov, Phys. Rev. B **32**, 755 (1985).

[5]M. P. Everson, A. Johnson, Hao-An Lu, R. V. Coleman, and L. M. Falicov, Phys. Rev. B **36**, 6953 (1987).

[6]For a review of the electronic properties of metals, see L. M. Falicov, *Electrons in Crystalline Solids* (IAEA, Vienna, 1973), p. 207.

[7]A. B. Pippard, Proc. R. Soc. London, Ser. A **270**, 1 (1962); Philos. Trans. R. Soc. London, Ser. A **256**, 317 (1964).

[8]R. G. Chambers, Proc. Phys. Soc. London **88**, 701 (1966); **89**, 695 (1966).

[9]L. M. Falicov, A. B. Pippard, and P. R. Sievert, Phys. Rev. **151**, 498 (1966).

[10]C. E. T. Gonçalves da Silva and L. M. Falicov, Phys. Rev. B **8**, 527 (1973).

[11]It should be noticed that interference effects in MB linked-orbit networks have been studied in detail for the case of Mg, Zn, and Cd for magnetic fields perpendicular to the hexagonal axis by R. W. Stark and R. Reifenberger, J. Low Temp. Phys. **26**, 763 (1977); **26**, 818 (1977).